J Appl Electrochem (2009) 39:2315–2321
DOI 10.1007/s10800-009-9954-7

REVIEW ARTICLE

Electrochemical behavior of aluminum in 1-*n*-butyl-3-methylimidazolium tetrafluoroborate ionic liquid electrolytes for capacitor applications

F. Trombetta · M. O. de Souza · R. F. de Souza · E. M. A. Martini

Received: 16 February 2009 / Accepted: 8 June 2009 / Published online: 21 June 2009

Abstract This study compares two series of solvents for application in aluminum electrolytic capacitors: ethylene glycol (EG) and water mixtures, and ethylene glycol and 1-*n*-butyl-3-methylimidazolium tetrafluoroborate ($BMI.BF_4$) ionic liquid (IL) mixtures. Electrochemical impedance spectroscopy and cyclic voltammetry were carried out with a previously anodized aluminum disk electrode. Comparative measurements of solution resistance, polarization resistance, AC capacitance, and passive current were made. The results show that EG–IL mixtures with low amounts of IL (10% IL–90% EG v/v) have a low solution resistance. Low values of solution resistance, high values of polarization resistance, small passive current, and uniform capacitance of anodized aluminum in EG–IL mixtures are favorable properties of the $BMI.BF_4$ IL for use as an electrolyte in the construction of electrolytic aluminum capacitors.

Keywords Electrolytic capacitors · Ionic liquids · Electrochemical impedance · Aluminum oxide · Ethylene glycol

1 Introduction

Aluminum electrolytic capacitors have received much attention due to their widespread use in electronic equipment. Their high capacitance per unit volume enables the construction of reduced-size capacitors in chip format [1, 2]. A conventional electrolytic capacitor consists of a sheet of aluminum coated with a dielectric Al_2O_3 layer as the anode and another aluminum sheet as the cathode. A porous sheet of paper is typically used to separate the electrodes, and all of the components are wound together. The roll is then impregnated with an electrolytic solution that usually contains ethylene glycol (EG), ammonium salts, and corrosion inhibitors.

Today, low impedance chip-type capacitors are required for miniaturized electronic equipment. Decreased impedance is attained by lowering the in-series resistance of the capacitor by increasing the conductivity of the electrolyte. Such conditions are difficult to obtain in an organic solvent, but can be reached via the addition of water to the capacitor electrolyte. However, the presence of water can cause technical problems due to both the narrow electrochemical window of water and the high temperatures involved in fabrication of the capacitor, which includes a heat sealing process. The formation of water vapor upon heating can contribute to the rupturing of the capacitor. Moreover, in commercial capacitors, the aluminum oxide can contain failures, requiring reformation to restore the oxide to its original state. This reforming oxidation process induces the reduction of water in the cathode by H_2 and OH^- production. The H_2 pressure can create a high internal pressure in the capacitor, which can lead to rupture. Furthermore, the hydroxyl ions locally increase the pH, and the aluminum oxide can react to form soluble aluminates [3], according to the following expression:

$$\gamma\text{-}Al_2O_{3(s)} + H_2O \rightarrow 2AlO_2^- + 2H^+. \quad (1)$$

These problems encourage investigations devoted to the development of non-aqueous electrolytes with high conductivity [4–19]. The key characteristics of ionic liquids are high decomposition voltage limits, wide

F. Trombetta · M. O. de Souza · R. F. de Souza · E. M. A. Martini (✉)
Institute of Chemistry, UFRGS, Av. Bento Gonçalves, 9500, P.O. Box 15003, Porto Alegre 91501-970, Brazil
e-mail: emilse@iq.ufrgs.br

ranges of operational temperatures, high ionic conductivities, non-corrosive nature [2], and making them attractive alternatives to water.

In this study, two series of solvents are compared as constituents in aluminum electrolytic capacitors: ethylene glycol and water mixtures (EG–H_2O) and ethylene glycol and 1-*n*-butyl-3-methylimidazolium tetrafluoroborate ($BMI.BF_4$) ionic liquid (IL) mixtures (EG–IL). Comparative measurements of solution resistance, polarization resistance, AC capacitance, and passive current were made.

2 Experimental

The working electrode consisted of a pure aluminum disk (99.999%, purchased from Goodfellow) inserted in a Teflon holder with an exposed area of 0.28 cm^2. The disk was polished with 400 and 600 grit emery papers and washed with water. The electrode was then immersed in a 1 M NaOH solution to dissolve any films that were previously formed in air, and washed with distilled water and alcohol prior to drying. The electrode was subsequently introduced to a 0.10 M $Na_2B_4O_7{\cdot}10H_2O$ (Borax) and NaH_2PO_4 aqueous solution and kept at a potential of 2 V (SCE) for 1 h to promote the growth of oxide film. The reference electrode was a saturated calomel electrode (SCE), and the counter electrode was a Pt wire. The charge density passed during the anodic oxidation was 70 ± 5 mC cm^{-2}. For similar charge densities, the thickness of the oxide may be considered as constant for all the experiments.

The anodized electrode was then dried and immersed in the electrochemical measurement solutions. Two different solvent systems were tested and compared: (1) ethylene glycol and water mixtures (EG–H_2O) and (2) ethylene glycol and 1-*n*-butyl-3-methylimidazolium tetrafluoroborate ($BMI.BF_4$) ionic liquid (IL) mixtures (EG–IL). $BMI.BF_4$ IL was prepared according to the previously published procedures [20, 21]. The ionic liquid was synthesized under Argon atmosphere and dried under reduced pressure. The solvent systems contained between 10% and 100% EG by volume. The salts $Na_2B_4O_7{\cdot}10H_2O$ and NaH_2PO_4 were used as solute in a concentration of 0.10 M. Electrochemical impedance spectroscopy measurements were performed at a potential of 1 V, over a frequency range of 100 mHz to 10 kHz, and at an amplitude of 10 mV. Cyclic voltammetric experiments were then performed. The electrode potential scan rate was set to 0.010 V s^{-1}, and the potential was scanned between the limits of -2 and $+2$ V (QSR); the first scan was recorded. The electrochemical measurements were carried out with an Autolab model PGSTAT 30 potentiostat coupled with a frequency response analyzer (FRA 2) for impedance spectroscopy and with a GPES module for cyclic voltammetry. The analytical cell consisted of a traditional three-electrode cell using a Pt wire as the quasi-reference electrode (QSR) and a Pt wire as the counter electrode. The electrochemical experiments were carried out in an open cell at regular atmosphere. Each experiment was conducted for approximately 1 h. The water content was determined using a coulometric Karl–Fischer titration (Titrino 756 KF Metrohm). After 1 h of exposure of IL to air, the water content attains only 0.02 wt%.

Analysis of impedance data is carried out over a wide frequency range with the aid of Nyquist complex plane plots or Bode plots to determine the individual components of an equivalent electrical circuit model that represents the aluminum/film/solution interfaces. The Nyquist complex plane plot graphs relate the resistive (Z') versus the reactive (Z'') components of impedance, Z. The Bode plot graphs relate the logarithm of the modulus of impedance, log |Z|, and the phase angle, θ, versus the logarithm of frequency, f. The intersection of the Nyquist arc with the resistive axis corresponds to the resistance values of the system. The same values can also be obtained through a Bode plot (log |Z| vs. log f), where the total impedance is constant in relation to the frequency. The capacitance can be obtained by the equation $C = (2\pi f Z)^{-1}$, where f is the frequency of the maximum value of phase angle in the Bode plot (phase angle vs. log f) and Z is the related impedance from the Bode plot (log |Z| vs. log f).

The experiments were carried out at room temperature. A new oxide film was created via polarization for each solvent mixture.

Analysis of electrode surfaces was made using scanning electronic microscopy (SEM) (JEOL-JSM 6060) with a voltage acceleration of 20 kV and a magnitude of 120.

3 Results and discussion

Electrochemical impedance spectroscopy was carried out to characterize the capacitive behavior of oxide-covered aluminum using EG–H_2O or EG–IL as the liquid contact. Figure 1 shows Nyquist (Fig. 1a) and Bode (Fig. 1b) impedance diagrams obtained with anodized aluminum in EG–H_2O mixtures.

The Nyquist diagram shows an incomplete arc in the analyzed frequency range. Two time constants were identified from the two maxima observed in the θ (phase angle) versus log f representation in the Bode diagram. The capacitive behavior of the system is reflected in the measured phase angle of close to 90° in the intermediate frequency range. An equivalent circuit was fitted to the experimental data as shown in Fig. 1a. This circuit was chosen both to minimize the number of circuit elements used to model the phenomena likely occurring at the electrode and to reasonably fit the experimental data.

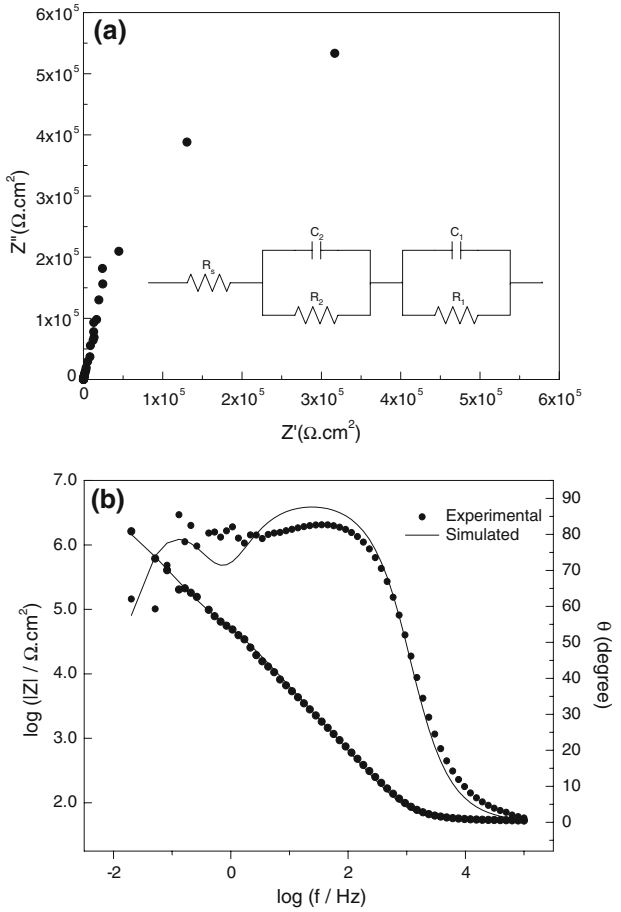

Fig. 1 Experimental and simulated Nyquist (**a**) and Bode (**b**) impedance diagrams of passivated aluminum at 1 V (QSR) in 0.1 M NaH_2PO_4 and borax solution. The solvent system is 50% (v/v) ethylene glycol and 50% (v/v) water

The components of the circuit represent the system characteristics as follows. R_S is the solution resistance. The parallel elements (R_1C_1) and (R_2C_2), arranged in series, are associated with a film composed of two superposed layers. The first layer, close to the metal, corresponds to a more compact material, such as an Al_2O_3 barrier, and is responsible for the highest potential drop. The second layer, close to the solution, corresponds to a more porous and less resistant compound, such as a porous hydrated oxide like $Al(OH)_3$ or AlOOH (bohemite) [22–24].

The total capacitance of the system, C_T, is the sum of the oxide capacitance (C_1) and the capacitance of the hydrated aluminum compounds (C_2) arranged in series. This C_T is related to the dielectric properties of the bilayer film.

The resistance polarization, R_P, corresponds to the sum of R_1 and R_2 arranged in series, i.e., to the sum of the resistance of each layer of the dielectric film. Since the systems studied are formed by a three-dimensional heterogeneous oxide layer, R_P is a complex function of the electrochemical reaction rate and of the mass transfer through the solid [23].

The experiments employing the EG–H_2O electrolyte mixtures were performed to compare the behavior of a traditional aluminum electrolytic capacitor with that of the EG–IL system, i.e., a non-aqueous mixture. This non-aqueous system is comprised EG, $BMI.BF_4$, borax, and sodium dihydrogenophosphate. The salts were added to the EG–IL mixtures to be sure that any change in the aluminum electrode behavior could be exclusively attributed to the substitution of water by $BMI.BF_4$.

Similar to that used in the traditional system, the electrode was dried and transferred to the EG–IL solutions after 1 h of anodization to form an oxide layer. Impedance measurements were made twice, the first immediately after the immersion of the electrode and the second after 1 h of immersion. This procedure was adopted to determine the wetting factor of the electrode as a result of the viscosity of the EG–IL medium, which has a higher viscosity than EG–H_2O solutions. Figure 2 shows the Nyquist (Fig. 2a) and

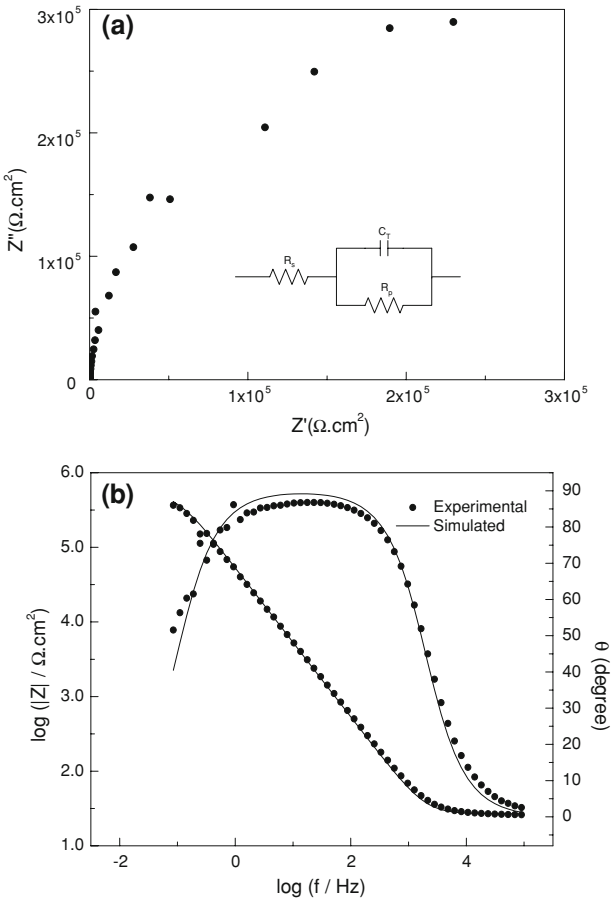

Fig. 2 Experimental and simulated Nyquist (**a**) and Bode (**b**) impedance diagrams of passivated aluminum at 1 V (QSR) in 0.1 M NaH_2PO_4 and borax solution. The solvent system is 50% (v/v) ethylene glycol and 50% (v/v) $BMI.BF_4$

Bode (Fig. 2b) diagrams obtained for aluminum in the EG–IL solutions.

The Nyquist diagram shows an incomplete capacitive arc (Fig. 2a). The Bode diagram of θ (phase angle) versus log f in the intermediate frequency range exhibits a broad peak at about 90° (Fig. 2b). The experimental data were fitted to an equivalent circuit, as shown in Fig. 2a. R_S is the solution resistance, R_P is the polarization resistance of the oxide coating on the electrode, and C_T is the capacitance associated with the dielectric oxide. The R_S for both the solvent systems are compared in Fig. 3. In the first system (EG–H_2O), the R_S, increases with increase in the EG concentration, indicating a decrease in the conductivity of the solution. The solution prepared with only EG exhibited slight turbidity, likely due to the hard salts dissolved in this medium. With the addition of water, the viscosity and turbidity of the solutions decreased. The added water also increased the electrolytic solution conductivity, due to increased salt dissolution and increased ion mobility. Values of R_S obtained for the EG–IL system are lower than those obtained for the EG–H_2O system, indicating that not only were the borate and phosphate salts dissociated, but that IL was also dissociated. The dissociated BMI cations and BF_4 anions are responsible for the increase in the conductivity of the solution.

Comparing the R_S of the EG–H_2O and EG–IL solutions in Fig. 3, it is interesting to note that the resistance of the EG–IL solution with only 10% IL v/v (or 90% EG v/v) is as low as that of the EG–H_2O solution with 70% v/v or more water. Such high water content corresponds to very unfavorable conditions for capacitor fabrication. These results are caused by the high IL solubility in EG and show that it is plausible to use an IL as the electrolyte for the fabrication of chip-type capacitors with low impedance.

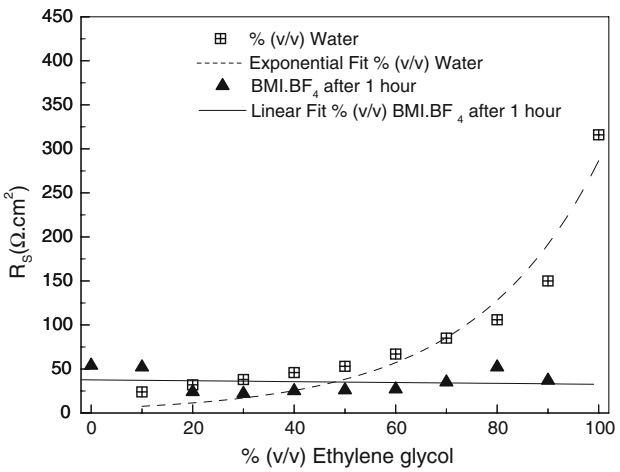

Fig. 3 A plot of the solution resistance (R_S) in function of volumetric percentage of ethylene glycol for passivated aluminum in ethylene glycol and water mixtures (⊠) and ethylene glycol and $BMI.BF_4$ mixtures (*filled triangle*)

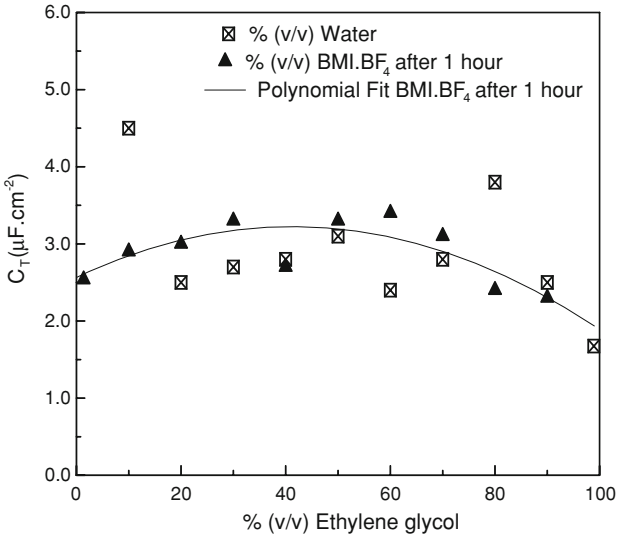

Fig. 4 A plot of the capacitance (C_T) in function of the volumetric percentage of ethylene glycol for passivated aluminum in ethylene glycol and water mixtures (⊠) and ethylene glycol and $BMI.BF_4$ mixtures (*filled triangle*)

Figure 4 shows the C_T of the dielectric layer on aluminum in different solvent systems. In the EG–H_2O environment, the C_T does not show a marked variation with changes in the mixture composition. Its value (1.7–4.5 μF cm^{-2}) is lower than the characteristic capacitance of an electric double layer for a metal without oxide, which is typically between 30 and 100 μF cm^{-2} [13], confirming the presence of an oxide layer coating the aluminum. In the EG–IL systems, the experimental capacitances (C_T) were similar to the values obtained for the EG–H_2O solutions, but more uniform over the range of EG–IL solution compositions (Fig. 4). Since the separation of charges occurs at the dielectric/solution interface, the solution is considered the true cathode in an electrolytic capacitor. It is important to observe that the time constant (R_2C_2) associated with the porous and hydrated layer in the EG–H_2O systems (Fig. 1) is absent or coupled to (R_1C_1) in the EG–IL systems, resulting in the time constant (R_PC_T) (Fig. 2). Then, in the EG–IL medium, the oxide film on the Al is consisted for only Al_2O_3, compact near to the metal and porous in the interface with the electrolyte, but not hydrated. The compact layer and the porous layer properties and dimensions are not substantially different to produce two time constants in the impedance results. These results show that the dielectric oxide is stable in the presence of the IL.

Figure 5 shows that the R_P measured in EG–IL mixtures (50% or less IL v/v) are higher than those measured in EG–H_2O systems. This result indicates that under the experimental conditions examined, the oxide layer is more stable in EG–IL solutions than in EG–H_2O solutions.

Furthermore, the stability of a capacitor can be evaluated through its sparking voltage (the voltage limit

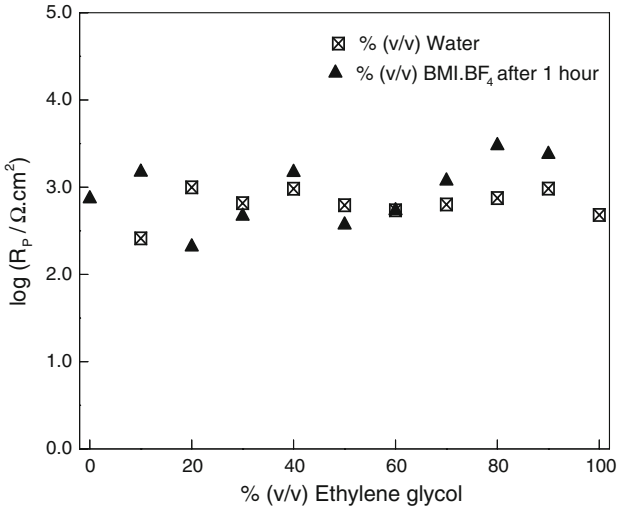

Fig. 5 A plot of the polarization resistance (R_P) in function of the volumetric percentage of ethylene glycol for passivated aluminum in ethylene glycol and water mixtures (⊠) and ethylene glycol and $BMI.BF_4$ mixtures (*filled triangle*)

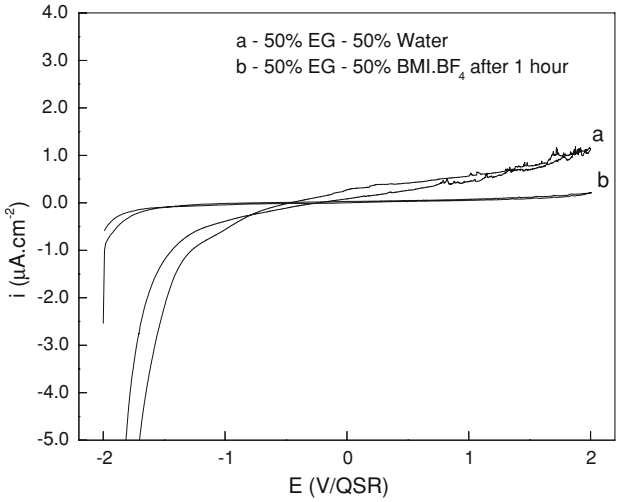

Fig. 6 Cyclic voltammograms of passivated aluminum in 0.1 M NaH_2PO_4 and borax solution. The solvent systems are 50% (v/v) ethylene glycol and 50% (v/v) water (a), and 50% (v/v) ethylene glycol and 50% (v/v) $BMI.BF_4$. The potential scan rate is 0.010 V s^{-1}

corresponding to the rupture of the capacitor when an anodic current is applied). Rupture of capacitors is typically caused by penetration of negative charges inside the oxide layer [1] to balance the negative charge deficit at the metal/oxide interface due to metal oxidation. The polarization resistance also contributes to the size of the sparking voltage. The R_P value increases with the increasing voltage drop through the film, making oxidation of the metal at the interface with the dielectric film more difficult.

After 1 h of immersion, the relatively constant value of C_T and the high value of R_P demonstrate the stability of the oxide layer formed in the EG–IL solutions tested (see Figs. 4, 5, respectively). The values of R_S did not change with the immersion time.

After each impedance experiment, a voltage scan from −2 to +2 V (QSR) was performed to investigate the electrochemical stability of the oxide in various media. Figure 6 shows a voltammogram obtained for the EG–H_2O mixture (50% EG v/v).

The limit current for the highest cathodic potential corresponds to the following reaction:

$$2H_2O + 2e^- \rightarrow H_2 + 2OH^-. \quad (2)$$

With increasing potential in the anodic range, no active current peak was recorded, demonstrating the passivity of the metal. The small anodic current that is recorded in the system, which increases with the potential, is equal to the sum of two terms: the capacitive current, responsible for charging the different interfaces, and the Faradaic current, which corresponds to the charge transfer reaction, i.e., the oxidation of Al to Al^{3+} that occurs at the Al/oxide interface. This oxidation leads to an increase in the layer thickness and also characterizes the leakage current of the capacitor. As the water content increases, the passive current and the cathodic current of H_2 evolution increase.

Similarly, for the traditional electrolyte mixture, voltage scanning was performed to investigate the electrochemical stability of the previously formed oxide layer in several EG–IL solutions. Figure 6 shows a voltammogram obtained for the EG–IL mixture (50% EG v/v). There was no active zone recorded in the anodic potential range, indicating the passivity of the electrode. The anodic current, which was constant with increases in potential, probably has mainly a capacitive contribution since the $BMI.BF_4$ electrochemical window is within the 4–6 V range when Pt electrodes are used [9]. As the amount of IL increases, the passive current increases, although less than in EG–H_2O systems. During the anodic polarization, the faradaic current is due to oxidation of the Al to Al^{3+} at the interface metal/oxide. Comparing the voltammograms (Fig. 6), in EG–IL medium, this oxidation occurs at a lower rate because the anhydrous and crystalline oxide show greater barrier effect making difficult the movement of the ions and vacancies across the film assisted by the local electrical field. The lower values of the anodic currents obtained for EG–IL mixtures (see Fig. 6) compared to those of the EG–H_2O mixtures confirm the stability of the oxide layer in this environment.

This study proves that EG–IL solvent systems show low R_S, which contributes to the decrease in the total impedance, a requirement for chip-type capacitors. Furthermore, EG–IL mixtures show uniform capacitance (Fig. 4), high polarization resistances (Fig. 5), and few microamperes of anodic current (Fig. 6); these properties attest to the aluminum dielectric oxide stability in this environment, which

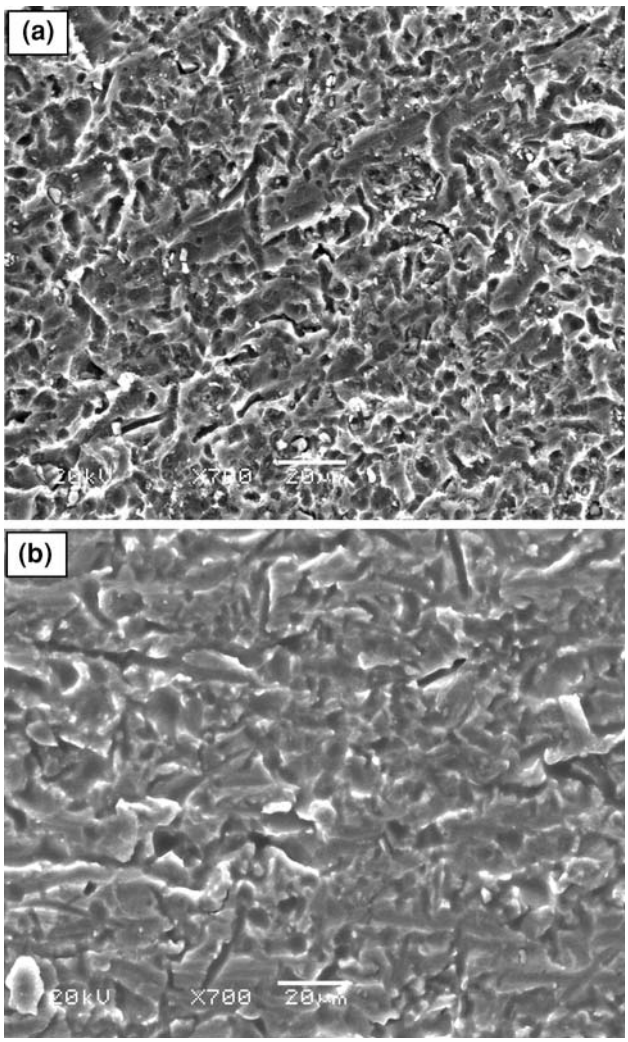

Fig. 7 SEM photographs of the anodized aluminum **a** without immersion and **b** after 5 days of immersion in 0.1 M NaH_2PO_4 and borax solution. The solvent is 100% (v/v) $BMI.BF_4$

is required for electrolytic capacitors. Our results demonstrate that the use of a non-aqueous IL solution as the electrolyte for electrolytic capacitor fabrication is a promising method for reducing the electrolytic R_S without adding water.

Figure 7 shows the SEM analyses of anodized aluminum electrode without immersion and after a 5-day immersion period in 100% IL v/v. Porous oxide layer is observed at both photographs. There is no localized corrosion of the surface; therefore, IL presents an additional and favorable property for use as electrolyte for aluminum electrolytic capacitor.

4 Conclusion

1-*n*-Butyl-3-methylimidazolium tetrafluoroborate is a non-volatile IL that shows high conductivity and electrochemical stability over a large range of potentials. The use of $BMI.BF_4$ as a non-aqueous electrolyte for traditional electrolytic aluminum capacitors is proposed in this study. Comparison of the performance of the anodized aluminum with a traditional aqueous electrolyte and that with $BMI.BF_4$ shows the following four advantages for the IL: (1) lower R_S (high conductivity), (2) higher polarization resistance, (3) uniform capacitance and (4) lower passive current, which can be associated with current leakage. These factors confirm the stability of the dielectric oxide in $BMI.BF_4$ environments.

The results show that a low R_S, as required for low impedance chip-type capacitors, is obtained in EG–IL solutions with only 10% IL v/v, while EG–H_2O solutions with 70% water v/v are required to achieve similar performance.

The results described herein show that $BMI.BF_4$ ionic liquid is promising for use in the construction of aluminum electrolytic capacitors as a component of the impregnation electrolyte.

Acknowledgments Fundação de Amparo à Pesquisa do Estado do Rio Grande do Sul (Fapergs/Pronex), Coordenação de Aperfeiçoamento de Pessoal de Nível Superior (CAPES), Conselho Nacional de Pesquisa (CNPq) and Centro de Microscopia Eletrônica (CME—UFRGS) are acknowledged for their contributions.

References

1. Song Y, Zhu X, Wang X, Wang M (2006) J Power Sources 157:610
2. Ue M (2000) Curr Top Electrochem 2:49
3. Pourbaix M (1963) Atlas d'équilibries eletroquimiques. Gautier-Villares, Paris
4. Galinski M, Lewandowski A, Stephniak I (2006) Electrochim Acta 51:5567
5. Tsuda T, Hussey CL (2007) Electrochem Soc Interface 16:42
6. Greaves TL, Drummond CJ (2008) Chem Rev 108:206
7. Wei D, Ivaska A (2008) Anal Chim Acta 607:126
8. Markevich E, Baranchugov V, Aurbach D (2006) Electrochem Commun 8:1331
9. de Souza RF, Loget G, Padilha JC, Martini EMA, de Souza MO (2008) Electrochem Commun 10:1673
10. Arbizzani C, Beninati S, Lazzari M, Soavi F, Mastragostino M (2007) J Power Sources 174:648
11. Ania CO, Pernak J, Stefania KF, Raymundo-Piñero E, Béguin F (2006) Carbon 44:3113
12. Yuyama K, Masuda G, Yoshida H, Sato T (2006) J Power Sources 162:1401
13. Sato T, Masuda G, Takagi K (2004) Electrochim Acta 49:3603
14. Zhu Q, Song Y, Zhu X, Wang XJ (2007) Electroanal Chem 601:229
15. Nagao Y, Nakayama Y, Oda H, Ishikawa M (2007) J Power Sources 166:595
16. Lewandowski A, Swiderska A (2006) Appl Phys A 82:579
17. Lewandowski A, Galinski M (2006) In: Barsukov IV, Johnson CS, Doninger JE, Barsukov VZ (eds) New carbon based materials for electrochemical energy storage systems. Springer, Netherlands, p 73
18. Franckowiak E (2006) J Braz Chem Soc 17:1074

19. Balducci A, Bardi U, Caporali S, Mastragostino M, Soavi F (2004) Electrochem Commun 6:566
20. Suarez PAZ, Dullius JEL, Einloft S, de Souza RF, Dupont J (1996) Polyhedron 15:1217
21. Dupont J, Consorti CS, Suarez PAZ, de Souza RF (2002) Org Synth 79:236
22. Metikos-Hukovic M, Babic R, Grubac Z, Brinic S (1994) J Appl Electrochem 24:772
23. Metikos-Hukovic M, Babic R, Grubac Z (2002) J Appl Electrochem 32:35
24. Juttner K, Lorenz WJ, Paatsch W (1989) Corros Sci 29:279